J Wood Sci (2011) 57:56–65
DOI 10.1007/s10086-010-1132-3

ORIGINAL ARTICLE

**Yuhua Bai · Ming Zhao · Liming Bai · Ryo Hasegawa
Jun-ichi Sakai · Toshiaki Hasegawa · Tomokazu Mitsui
Hirotsugu Ogura · Takao Kataoka · Katsutoshi Hirose
Masayoshi Ando**

The biological activities of cardenolide triglycosides from stems, twigs, and leaves of *Nerium oleander*

Received: February 4, 2010 / Accepted: April 28, 2010 / Published online: August 5, 2010

Abstract Sixteen cardenolide triglycosides (**1**–**16**) were isolated from stems, twigs, and leaves of *Nerium oleander*. Among them, 3*β*-*O*-(4-*O*-gentiobiosyl-D-diginosyl)-7*β*,8-epoxy-14-hydroxy-5*β*,14*β*-card-20(22)-enolide, named cardenolide B-3 (**16**), was isolated from natural sources for the first time. The in vitro anti-inflammatory activities of compounds **1**–**16** were examined on the basis of inhibitory activity against the induction of intercellular adhesion molecule-1 (ICAM-1). Compounds **1**–**5** were active at an IC_{50} value of less than 7 μM. The cytotoxic activity of isolated compounds was evaluated against three human cell lines: normal human fibroblast cells (W-38), malignant tumor cells induced from WI-38 (VA-13), and human liver tumor cells (HepG2). Compounds **1**–**5** were active toward WI-38 cells; compounds **1**, **3**, and **5** were active toward VA-13 cells; and compounds **1**–**5** were active toward HepG2 cells at IC_{50} values of less than 10 μM. The multidrug-resistant (MDR) cancer-reversal activity of compounds **1**–**16** was evaluated on the basis of the amount of calcein accumulated in MDR human ovarian cancer 2780AD cells in the presence of each compound. Compounds **13** and **14** showed significant effects on calcein accumulation.

Key words *Nerium oleander* · Cardenolide triglycosides · Anti-inflammatory activity · Cytotoxic activity · Multidrug-resistant (MDR) cancer-reversal activity · Cardenolide B-3

Y. Bai (✉)
Department of Pharmacy, Daqing Campus of Harbin Medical University, Daqing Hi-Tech Development Zone, Xinyang Road, Daqing 163319, China
Tel. +86-459-8977566; Fax +86-459-8153201
e-mail: b_yuhua@yahoo.com

M. Zhao · L. Bai
College of Chemistry and Chemistry Engineering, Qiqihar University, Qiqihar 161006, China

R. Hasegawa
Graduate School of Science and Technology, Niigata University, Niigata 950-2181, Japan

J. Sakai · M. Ando
Department of Chemistry and Chemical Engineering, Niigata University, Niigata 950-2181, Japan

T. Hasegawa
Niigata Research Laboratory, Mitsubishi Gas Chemical Company, Inc., Niigata 950-3112, Japan

T. Mitsui · H. Ogura · T. Kataoka
Center for Biological Resources and Informatics, Tokyo Institute of Technology, Yokohama 226-8501, Japan

K. Hirose
KNC Laboratories Co. Ltd., Kobe 651-2271, Japan

Introduction

Nerium oleander is a medium-sized (2–5 m in height) evergreen flowering tree and is planted throughout Japan as a garden and roadside tree. Cardenolides of this plant were investigated because of the interest in their biological activities.[1] The cardiac glycosides digitoxin and digoxin have been used in treatment of cardiac diseases for many years.[1,2] Anticancer utilization of digitoxin, digoxin, and related cardenolides has also been investigated.[3,4] We recently took a fresh look at the bioactive cardenolides[5] and pregnanes[6] of *N. oleander* and investigated their biological activities. Further investigation of the chemical constituents of stems, twigs, and leaves resulted in a new cardenolide triglycoside, cardenolide B-3 (**16**), and fifteen known cardenolide triglycosides **1**–**15** (Fig. 1). We report here their biological activities such as anti-inflammatory activity, cytotoxic activity toward human tumor cells, and multidrug-resistant (MDR) cancer-reversal activity.

Experimental

The instrumentation and chromatography were the same as described previously.[5,6]

Plant material

The stems, twigs, and leaves of *N. oleander* were collected in Niigata City, Niigata Province, Japan, in November 2001.

Fig. 1. Cardenolide triglycosides from *Nerium oleander*

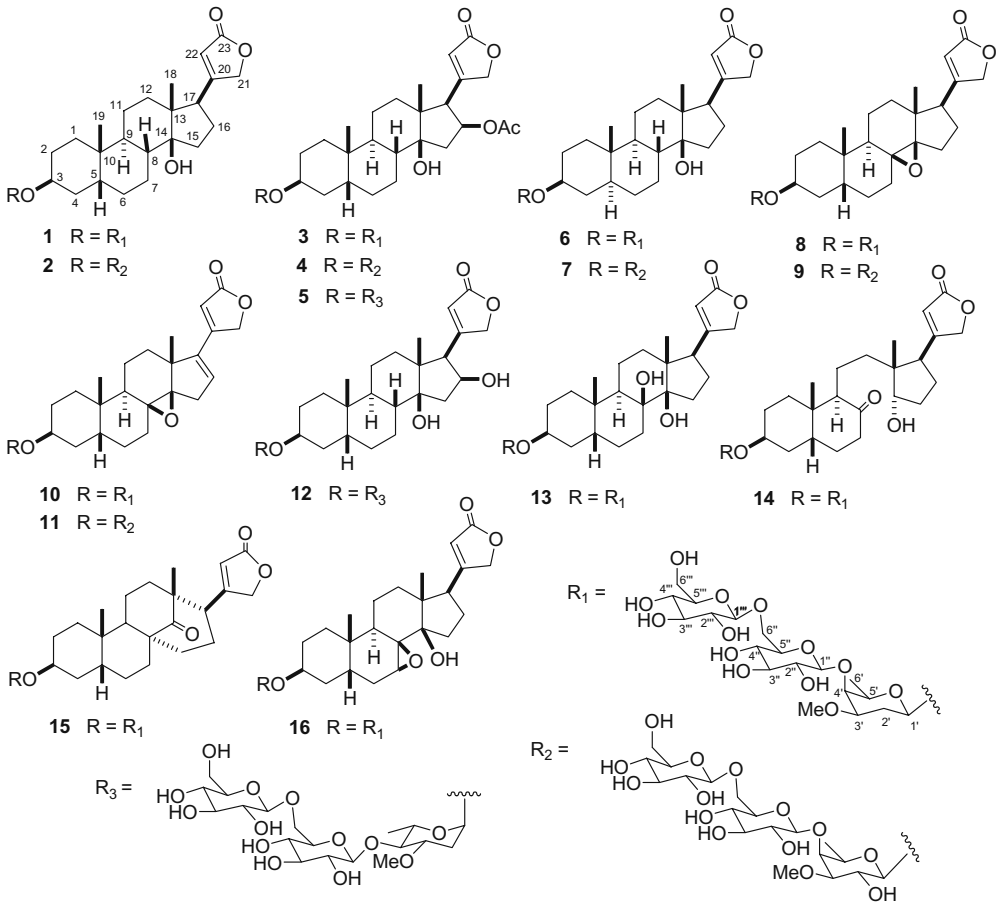

The plant was identified by Dr. K. Yonekura, Department of Biology, Faculty of Science, Tohoku University, Sendai, Japan. A voucher specimen (2001-11-10) was deposited at the Department of Chemistry and Chemical Engineering, Niigata University.

Extraction and isolation

From stems and twigs. The *n*-butanol extract (244 g) was obtained from air-dried stems and twigs (19.46 kg) of *N. oleander* by the extraction procedures shown in Fig. 2. This material was separated by a combination of column chromatography [silica gel, gradient ($CHCl_3$–MeOH)] and reversed-phase HPLC [ODS, gradient (MeOH–CH_3CN–H_2O)] by the separation procedures shown in Fig. 3. The isolated compounds and their yields were as follows: **1** [7.280 g (0.0374%)], **2** [12.630 g (0.0649%)], **3** [1.627 g (0.0084%)], **4** [2.307 g (0.0119%)], **5** [0.717 g (0.0037%)], **6** [1.036 g (0.0053%)], **7** [0.454 g (0.0023%)], **8** [2.860 g (0.0147%)], **9** (0.450 g (0.0023%)), **10** [0.482 g (0.0025%)], **11** [0.510 g (0.0026%)], **14** [0.741 g, (0.0038%)], **15** [1.977 g, (0.0102%)], **16** [0.162 g (0.0008%)].

From leaves. The *n*-butanol extract (528 g) was obtained from air-dried leaves (9.91 kg) of *N. oleander* by the extraction procedures shown in Fig. 4. This material was separated by a combination of column chromatography [silica gel, gradient ($CHCl_3$–MeOH–H_2O)] and reversed-phase HPLC [ODS, gradient (MeOH–CH_3CN–H_2O)] by the separation procedures shown in Fig. 5. The isolated compounds and their yields were as follows: **1** [280 mg (0.0028%)], **2** [142 mg (0.0014%)], **3** [277 mg (0.0028%)], **5** [1408 mg (0.0142%)], **8** [1166.2 mg (0.0118%)], **11** [60 mg (0.0006%)], **12** [115 mg (0.0012%)], **13** [147 mg (0.0015%)], **14** [237 mg, (0.0024%)], **15** [786 mg, (0.0079%)].

Identification of isolated compounds

Cardenolide B-3 (**16**) was newly isolated by us from *N. oleander* and its structure determination was reported separately.[7] The physical constants and spectral data for the identification of **16** are described in this report.[7] Although the structures of **8** and **10** have already been reported by Yamauchi et al., their structure elucidation was based on products resulting from acid and enzymatic hydrolyses of a mixture of **8** and **10**.[8] Since we isolated **8** and **10** in pure form in this work, their structures were confirmed by the analyses of ^{1}H- and ^{13}C-NMR spectra including ^{1}H-^{1}H correlation spectroscopy (^{1}H-^{1}H COSY), distortionless enhancement by polarization transfer (DEPT), heteronuclear multiple quamtum coherence (HMQC), heteronuclear multiple bond coherence (HMBC), and nuclear overhauser

effect spectroscopy (NOESY) experiments. The physical constants and NMR and IR spectroscopic data for **8** and **10** are given below.

3β-O-(4-O-Gentiobiosyl-D-diginosyl)-8,14-epoxy-5β,14β-card-20(22)-enolide.[8] **8** was obtained as colorless microcrystals; mp 201°–203°C (acetone-hexane); $[\alpha]_D^{20}$ +14.6° (*c* 0.125, MeOH). ^{1}H NMR (C_5D_5N) δ 6.04 (1H, br s, 22-H), 5.14 (1H, d, J = 7.8 Hz, 1‴-H), 5.05 (1H, d, J = 7.8 Hz, 1″-H), 4.91 (1H, dd, J = 17.5, 1.7 Hz, 21b-H), 4.81 (1H, dd, J = 17.5, 2.0 Hz, 21a-H), 4.77 (1H, m, 6″b-H), 4.64 (1H, dd, J = 9.6, 1.7 Hz, 1′-H), 4.48 (1H, m, 6‴b-H), 4.34 (1H, m, 6‴a-H), 4.31 (1H, m, 3-H), 4.28 (1H, m, 4′-H), 4.26 (1H, m, 6″a-H), 4.19 (1H, m, 4‴-H), 4.18 (1H, m, 3‴-H), 4.11 (1H, m, 3″-H), 4.04 (1H, m, 5″-H), 4.00 (1H, m, 2‴-H), 3.98 (1H, m, 4″-H), 3.91 (1H, m, 5‴-H), 3.87 (1H, m, 2″-H), 3.53 (1H, q, J = 6.3 Hz, 5′-H), 3.42 (1H, m, 3′-H), 3.35 (3H, s, OMe), 2.46 (1H, m, 17-H), 2.35 (1H, m, 2′b-H), 2.12 (1H, m, 2′a-H), 1.95 (1H, m,

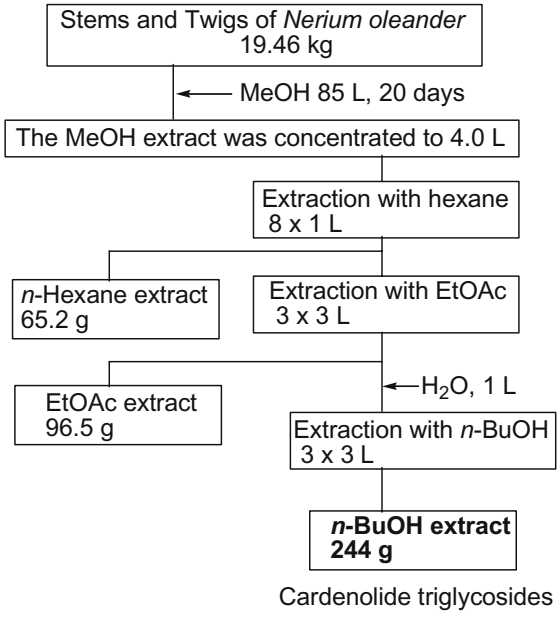

Fig. 2. Extraction procedures of the stems and twigs of *Nerium oleander*. *EtOAc*, ethyl acetate

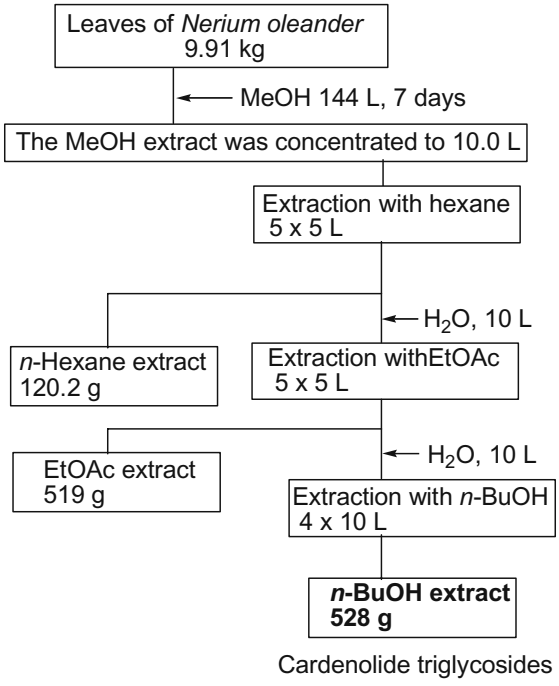

Fig. 4. Extraction procedures of the leaves of *Nerium oleander*

Fig. 3. Separation procedures of *n*-butanol extract of the stems and twigs of *Nerium oleander*

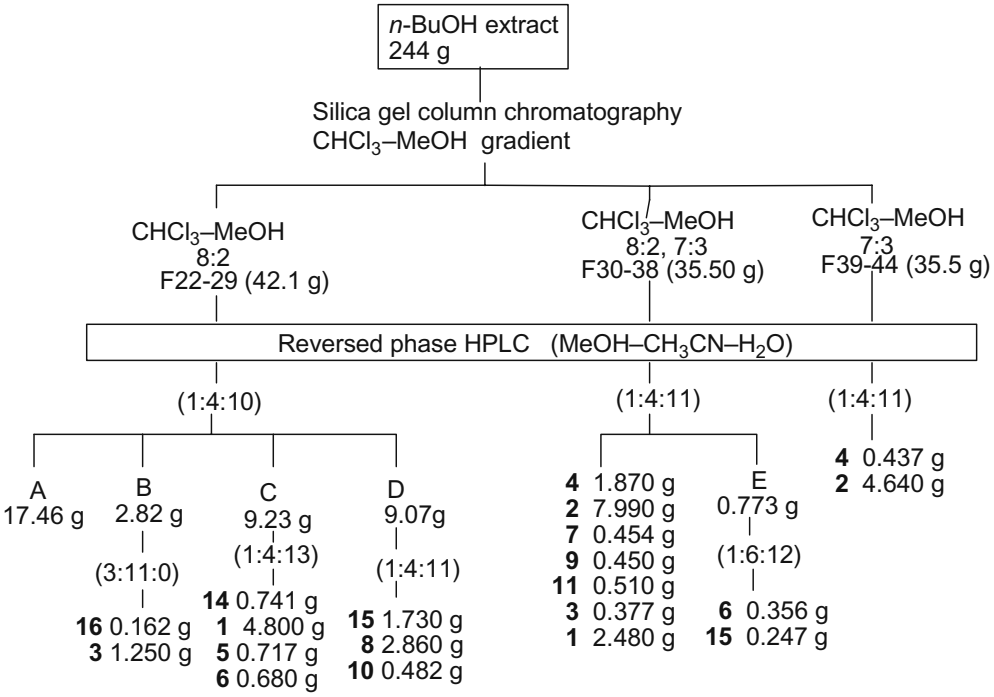

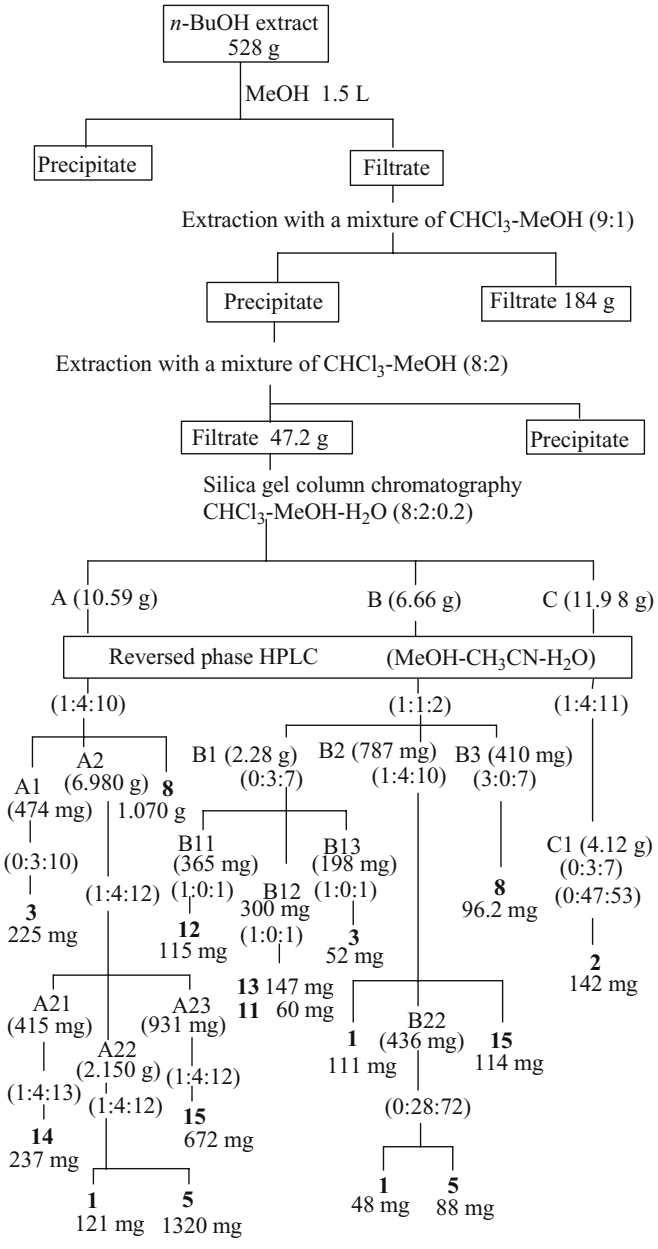

Fig. 5. Separation procedures of *n*-butanol extract of the leaves of *Nerium oleander*

5-H), 1.64 (1H, d, *J* = 6.3 Hz, 6′-H), 1.07 (3H, s, 19-H), 0.80 (3H, s, 18-H). ^{13}C NMR (C_5D_5N): see Table 1. IR (KBr): ν_{max} cm^{-1} 3404, 1747.

3β-O-(4-O-Gentiobiosyl-D-diginosyl)-8,14-epoxy-5β,14β-card-16,20(22)-enolide.[8] **10** was obtained as colorless microcrystals; mp 160°–163°C (acetone-hexane); $[\alpha]_D^{20}$ 22.8° (*c* 0.785, MeOH).^{1}H NMR (C_5D_5N) δ 6.28 (1H, m, 22-H), 6.08 (1H, br t, *J* = 2.8 Hz, 16-H), 5.15 (1H, d, *J* = 7.6 Hz, 1‴-H), 5.09 (1H, d, *J* = 7.8 Hz, 1″-H), 5.09 (1H, br dd, *J* = 16.2, 1.7 Hz, 21b-H), 5.05 (1H, br dd, *J* = 16.2, 1.7 Hz, 21a-H), 4.79 (1H, dd, *J* = 11.8, 1.7 Hz, 6″b-H), 4.68 (1H, br dd, *J* = 9.5, 2.0, 1′-H), 4.50 (1H, dd, *J* = 11.6, 2.4 Hz, 6‴b-H), 4.34 (1H, dd, *J* = 11.7, 5.4 Hz, 6‴a-H), 4.31 (1H, m, 4′-H), 4.29 (1H, m, 3-H), 4.27 (1H, m, 6″a-H), 4.21 (1H, m, 4‴-H), 4.18 (1H, m, 3‴-H), 4.12 (1H, m, 3″-H), 4.07 (1H, m, 5″-H), 4.02 (1H, m, 2‴-H), 3.98 (1H, m, 4″-H), 3.92 (1H, m, 5‴-H), 3.88 (1H, m, 2″-H), 3.52 (1H, q, *J* = 6.4 Hz, 5′-H), 3.42 (1H, m, 3′-H), 3.36 (3H, s, 3′-OMe), 2.36 (1H, m, 2′b-H), 2.12 (1H, m, 2′a-H), 1.95 (1H, m, 9-H), 1.92 (1H, m, 5-H), 1.65 (3H, d, *J* = 6.4 Hz, 6′-H), 1.24 (3H, s, 18-H), 1.10 (3H, s, 19-H). ^{13}C NMR (C_5D_5N): see Table 1. IR (KBr): ν_{max} cm^{-1} 3452, 1746.

The structures of the known compounds **1**–**7**, **9**, **11**–**15** were confirmed by analyses of ^{1}H- and ^{13}C-NMR spectra, including H-H COSY, DEPT, HMQC, HMBC, and NOESY experiments as well as by comparison of their spectral data and physical data with those reported previously. The physical constants, IR spectroscopic data, and references are given below. For convenience in identification of the compounds, ^{13}C NMR spectroscopic data of compounds **1**–**16** are summarized in Table 1.

3β-O-(4-O-Gentiobiosyl-D-diginosyl)-14-hydroxy-5β,14β-card-20(22)-enolide.[8,9] **1** was obtained as a colorless powder; mp 175°–179°C (acetone–hexane); $[\alpha]_D^{20}$ –23.5° (*c* 0.625, MeOH). IR (KBr): ν_{max} cm^{-1} 3508, 1742.

3β-O-(4-O-Gentiobiosyl-D-digitalosyl)-14-hydroxy-5β,14β-card-20(22)-enolide.[8,10,11] **2** was obtained as a colorless powder; mp 172°–175°C (acetone–hexane); $[\alpha]_D^{20}$ –18.9° (*c* 0.730, MeOH). IR (KBr): ν_{max} cm^{-1} 3408, 1745.

3β-O-(4-O-Gentiobiosyl-D-diginosyl)-16β-acetoxy-14-hydroxy-5β,14β-card-20(22)-enolide.[12] **3** was obtained as a colorless powder; mp 180°–183°C (acetone–hexane); $[\alpha]_D^{20}$ –28.0° (*c* 0.596, MeOH). IR (KBr): ν_{max} cm^{-1} 3408, 1745.

3β-O-(4-O-Gentiobiosyl-D-digitalosyl)-16β-acetoxy-14-hydroxy-5β,14β-card-20(22)-enolide.[13] **4** was obtained as a colorless powder; mp 185°–190°C (acetone–hexane); $[\alpha]_D^{20}$ –18.3° (*c* 0.769, MeOH). IR (KBr): ν_{max} cm^{-1} 3418, 1738.

3β-O-(4-O-Gentiobiosyl-L-oleandrosyl)-16β-acetoxy-14-hydroxy-5β,14β-card-20(22)-enolide.[8] **5** was obtained as a colorless powder; mp 169°–173°C (acetone–hexane); $[\alpha]_D^{20}$ –60.9° (*c* 0.465, MeOH). IR (KBr): ν_{max} cm^{-1} 3354, 1738.

3β-O-(4-O-Gentiobiosyl-D-diginosyl)-14-hydroxy-5α,14β-card-20(22)-enolide (odoroside K).[9,14] **6** was obtained as a colorless powder; mp 166°–168°C (acetone–hexane); $[\alpha]_D^{20}$ –22.8° (*c* 0.654, MeOH); IR (KBr): ν_{max} cm^{-1} 3250, 1740.

*3β-O-(4-O-Gentiobiosyl-D-digitalosyl)-14-hydroxy-5α,14β-card-20(22)-*enolide.[10] **7** was obtained as a colorless powder; mp 170°–173°C (acetone–hexane); $[\alpha]_D^{29}$ –23.6° (*c* 0.585, MeOH). IR (KBr): ν_{max} cm^{-1} 3474, 1726.

3β-O-(4-O-Gentiobiosyl-D-digitalosyl)-8,14-epoxy-5β,14β-card-20(22)-enolide.[12] **9** was obtained as a colorless powder; mp 170°–172°C (acetone–hexane); $[\alpha]_D^{28}$ –20.6° (*c* 0.631, MeOH). IR (KBr): ν_{max} cm^{-1} 3303, 1746.

3β-O-(4-O-Gentiobiosyl-D-digitalosyl)-8,14-epoxy-5β,14β-card-16,20(22)-enolide.[12] **11** was obtained as a colorless powder; mp 181°–184°C (acetone–hexane); $[\alpha]_D^{20}$ +28.5° (*c* 0.260, MeOH). IR (KBr): ν_{max} cm^{-1} 3344, 1746.

3β-O-(4-O-Gentiobiosyl-L-oleandrosyl)-14,16β-dihydroxy-5β,14β-card-20(22)-enolide.[12] **12** was obtained as a colorless powder (acetone–hexane); mp 208°–211°C; $[\alpha]_D^{20}$ –41.0° (*c* 0.315, MeOH). IR (KBr): ν_{max} cm^{-1} 3431, 1728.

3β-O-(4-O-Gentiobiosyl-D-diginosyl)-8β,14-dihydroxy-5β,14β-card-20(22)-enolide.[12] **13** was obtained as a colorless powder (acetone–hexane); mp 181°–184°C; $[\alpha]_D^{20}$ –21.5° (*c* 0.455, MeOH). IR (KBr): ν_{max} cm^{-1} 3430, 1738.

Table 1. ^{13}C NMR data of cardenolide triglycosides **1–16** from *Nerium oleander* (C_6D_5N, 125 MHz, δ in ppm, J in Hz)

Position	1	2	3	4	5	6	7	8	9	10	11	12	13	14	15	16
1	30.7 (t)	30.5 (t)	30.7 (t)	30.6 (t)	31.1 (t)	37.4 (t)	37.4 (t)	31.0 (t)	30.9 (t)	30.8 (t)	30.7 (t)	31.1 (t)	32.4 (t)	30.8 (t)	31.9 (t)	31.9 (t)
2	27.0 (t)	27.1 (t)	27.1 (t)	27.0 (t)	26.8 (t)	30.1 (t)	30.0 (t)	27.4 (t)	27.4 (t)	27.3 (t)	27.3 (t)	26.9 (t)	27.5 (t)	27.2 (t)	27.2 (t)	27.6 (t)
3	73.0 (d)	74.4 (d)	73.6 (d)	74.4 (d)	72.0 (d)	78.5 (d)	77.3 (d)	73.6 (d)	74.2 (d)	72.9 (d)	74.2 (d)	72.0 (d)	72.8 (d)	74.5 (d)	72.8 (d)	72.4 (d)
4	30.3 (t)	30.7 (t)	30.5 (t)	30.5 (t)	30.5 (t)	34.9 (t)	34.7 (t)	30.3 (t)	30.4 (t)	30.4 (t)	30.4 (t)	30.1 (t)	30.5 (t)	30.6 (t)	30.5 (t)	33.1 (t)
5	35.8 (d)	36.7 (d)	37.0 (d)	36.6 (d)	35.8 (d)	44.5 (d)	44.5 (d)	36.7 (d)	36.7 (d)	37.2 (d)	36.7 (d)	37.1 (d)	37.4 (d)	36.7 (d)	37.4 (d)	32.0 (d)
6	27.3 (t)	27.2 (t)	27.0 (t)	27.0 (t)	27.1 (t)	30.0 (t)	29.2 (t)	27.3 (t)	27.4 (t)	25.3 (d)	27.1 (t)	27.2 (t)	28.6 (t)	27.2 (t)	24.6 (t)	28.4 (t)
7	22.0 (t)	21.6 (t)	21.7 (t)	21.6 (t)	21.2 (t)	28.1 (t)	28.0 (t)	25.2 (t)	25.1 (t)	27.2 (t)	25.1 (t)	22.0 (t)	23.4 (t)	38.2 (t)	29.3 (t)	51.1 (d)
8	41.8 (d)	42.0 (d)	42.0 (d)	42.0 (d)	41.8 (d)	41.8 (d)	41.7 (d)	65.2 (s)	65.2 (s)	65.1 (s)	65.1 (s)	42.2 (d)	76.8 (s)	216.4 (s)	48.9 (s)	64.5 (s)
9	37.0 (d)	36.0 (d)	35.9 (d)	35.9 (d)	37.1 (d)	50.0 (d)	50.0 (d)	37.1 (d)	37.0 (d)	36.3 (d)	36.3 (d)	35.8 (d)	36.8 (d)	51.3 (d)	46.0 (d)	34.4 (d)
10	35.5 (s)	35.5 (s)	35.5 (s)	35.4 (s)	35.5 (s)	36.1 (s)	36.1 (s)	37.1 (s)	37.0 (s)	31.7 (s)	37.0 (s)	35.5 (s)	35.8 (s)	42.7 (s)	37.6 (s)	34.0 (s)
11	21.5 (t)	22.0 (t)	21.2 (t)	21.4 (t)	21.7 (t)	21.6 (t)	21.5 (t)	16.5 (t)	16.5 (t)	16.1 (t)	16.0 (t)	21.4 (t)	18.3 (t)	27.7 (t)	21.3 (t)	21.0 (t)
12	39.8 (t)	40.0 (t)	39.0 (t)	39.0 (t)	39.0 (t)	39.7 (t)	39.7 (t)	36.7 (t)	36.8 (t)	33.4 (t)	33.4 (t)	40.2 (t)	40.7 (t)	35.2 (t)	42.6 (t)	40.9 (t)
13	50.1 (s)	50.2 (s)	50.5 (s)	50.5 (s)	50.5 (s)	50.1 (s)	50.0 (s)	41.8 (s)	41.5 (s)	45.0 (s)	45.0 (s)	50.6 (s)	50.9 (s)	51.3 (s)	47.5 (s)	52.7 (s)
14	84.6 (s)	84.7 (s)	83.5 (s)	83.4 (s)	83.5 (s)	84.6 (s)	84.6 (s)	70.8 (s)	70.7 (s)	70.3 (s)	70.3 (s)	84.2 (s)	85.9 (s)	79.4 (d)	221.3 (s)	81.8 (s)
15	33.1 (t)	33.2 (t)	41.3 (t)	41.3 (t)	41.3 (t)	33.2 (t)	33.2 (t)	26.9 (t)	26.8 (t)	33.4 (t)	33.3 (t)	44.0 (t)	35.3 (t)	27.2 (t)	44.0 (t)	35.4 (t)
16	27.2 (t)	27.4 (t)	75.0 (d)	74.9 (d)	75.0 (d)	27.3 (t)	27.3 (t)	25.9 (t)	25.9 (t)	132.9 (d)	132.9 (d)	72.4 (d)	27.5 (t)	18.3 (t)	26.9 (t)	28.8 (t)
17	51.4 (d)	51.5 (d)	56.8 (d)	56.8 (d)	56.8 (d)	51.5 (d)	51.5 (d)	51.4 (d)	51.4 (d)	143.3 (s)	143.3 (s)	59.4 (t)	52.3 (d)	46.3 (d)	52.9 (d)	51.0 (d)
18	16.2 (q)	16.2 (q)	16.3 (q)	16.3 (q)	16.3 (q)	16.2 (q)	16.2 (q)	16.3 (q)	16.3 (q)	20.1 (q)	20.1 (q)	17.0 (q)	18.6 (q)	17.6 (q)	23.3 (q)	17.4 (q)
19	23.9 (q)	23.7 (q)	23.9 (q)	23.7 (q)	24.0 (q)	12.2 (q)	12.2 (q)	25.0 (q)	24.8 (q)	24.9 (q)	24.7 (q)	24.1 (q)	26.2 (q)	23.8 (q)	26.4 (q)	24.5 (q)
20	176.0 (s)	175.9 (s)	170.2 (s)	169.7 (s)	169.7 (s)	175.9 (s)	174.5 (s)	170.6 (s)	170.6 (s)	158.5 (s)	158.5 (s)	172.4 (s)	175.7 (s)	172.5 (s)	171.8 (s)	175.1 (s)
21	73.7 (t)	73.7 (t)	76.2 (t)	76.2 (t)	76.2 (t)	73.7 (t)	73.7 (t)	73.6 (t)	73.6 (t)	71.8 (t)	74.2 (t)	76.7 (t)	73.7 (t)	76.4 (t)	73.4 (t)	73.7 (t)
22	117.6 (d)	117.7 (d)	121.6 (d)	121.6 (d)	121.7 (d)	117.7 (d)	117.7 (d)	116.9 (d)	116.9 (d)	113.2 (d)	113.1 (d)	120.2 (d)	117.7 (d)	116.8 (d)	116.3 (d)	117.8 (d)
23	174.5 (s)	174.5 (s)	174.1 (s)	174.1 (s)	174.1 (s)	174.5 (s)	175.9 (s)	173.8 (s)	173.9 (s)	174.5 (s)	174.5 (s)	174.6 (s)	174.4 (s)	174.1 (s)	173.8 (s)	174.4 (s)
16-OAc			170.0 (s) 20.7 (q)	170.2 (s) 20.7 (q)	170.2 (s) 20.7 (q)											
1′	98.7 (d)	103.4 (d)	98.9 (d)	103.4 (d)	96.0 (d)	98.3 (d)	102.4 (d)	98.8 (d)	103.5 (d)	98.9 (d)	103.5 (d)	95.7 (d)	98.7 (d)	99.0 (d)	98.8 (d)	98.9 (d)
2′	33.2 (t)	70.6 (d)	33.3 (t)	70.6 (d)	35.8 (t)	33.3 (t)	70.6 (d)	33.3 (t)	71.4 (d)	33.3 (t)	71.3 (d)	35.8 (t)	33.3 (t)	33.2 (t)	33.3 (t)	33.3 (t)
3′	80.1 (d)	85.7 (d)	80.2 (d)	85.6 (d)	79.4 (d)	80.2 (d)	85.6 (d)	80.2 (d)	85.7 (d)	80.2 (d)	85.7 (d)	79.4 (d)	80.2 (d)	80.2 (d)	80.1 (d)	80.2 (d)
4′	73.2 (d)	76.0 (d)	73.1 (d)	75.9 (d)	82.2 (d)	73.4 (d)	75.8 (d)	73.6 (d)	75.8 (d)	73.6 (d)	75.8 (d)	82.2 (d)	73.5 (d)	73.1 (d)	73.6 (d)	73.6 (d)
5′	70.8 (d)	71.4 (d)	70.9 (d)	71.3 (d)	67.8 (d)	70.9 (d)	71.4 (d)	70.9 (d)	70.6 (d)	71.0 (d)	70.6 (d)	67.8 (d)	70.9 (d)	70.9 (d)	70.9 (d)	71.0 (d)
6′	18.1 (q)	18.0 (q)	18.1 (q)	18.0 (q)	18.9 (q)	18.2 (q)	18.0 (q)	18.1 (q)	18.0 (q)	18.2 (q)	18.0 (q)	18.8 (q)	18.1 (q)	18.1 (q)	18.1 (q)	18.2 (q)
OMe	56.1 (q)	58.9 (q)	56.2 (q)	58.9 (q)	56.9 (q)	56.3 (q)	58.9 (q)	56.2 (q)	58.9 (q)	56.2 (q)	58.9 (q)	56.7 (q)	56.2 (q)	56.2 (q)	56.2 (q)	56.2 (q)
1″	104.5 (d)	105.2 (d)	104.6 (d)	105.1 (d)	105.0 (d)	104.6 (d)	105.1 (d)	104.7 (d)	105.1 (d)	104.7 (d)	105.1 (d)	105.0 (d)	104.6 (d)	104.5 (d)	104.7 (d)	104.7 (d)
2″	75.6 (d)	75.8 (d)	75.7 (d)	75.7 (d)	75.8 (d)	75.8 (d)	75.8 (d)	75.7 (d)	75.2 (d)	75.7 (d)	75.2 (d)	75.8 (d)	75.7 (d)	75.7 (d)	75.7 (d)	75.8 (d)
3″	78.2 (d)	78.4 (d)	78.5 (d)	78.3 (d)	78.4 (d)	78.4 (d)	78.6 (d)	78.3 (d)	78.4 (d)	78.4 (d)	78.5 (d)	78.3 (d)	78.3 (d)	78.3 (d)	78.4 (d)	78.4 (d)
4″	71.8 (d)	71.9 (d)	71.8 (d)	71.8 (d)	72.1 (d)	72.0 (d)	71.9 (d)	71.9 (d)	71.9 (d)	71.8 (d)	71.8 (d)	72.1 (d)	71.9 (d)	71.9 (d)	71.8 (d)	72.0 (d)
5″	77.6 (d)	77.7 (d)	77.6 (d)	77.7 (d)	77.3 (d)	77.7 (d)	77.7 (d)	77.6 (d)	77.7 (d)	77.7 (d)	77.7 (d)	77.3 (d)	77.6 (d)	77.7 (d)	77.6 (d)	77.7 (d)
6″	70.3 (t)	70.5 (t)	70.5 (t)	70.4 (t)	70.7 (t)	70.5 (t)	70.5 (t)	70.5 (t)	70.5 (t)	70.5 (t)	70.5 (t)	70.7 (t)	70.4 (t)	70.4 (t)	70.5 (t)	70.5 (t)
1‴	105.5 (d)	105.6 (d)	105,6 (d)	105.6 (d)	105.6 (d)	105.6 (d)	105.6 (d)	105.6 (d)	105.6 (d)	105.6 (d)	105.6 (d)	105.6 (d)	105.6 (d)	105.6 (d)	105.6 (d)	105.6 (d)
2‴	75.1 (d)	75.2 (d)	75.2 (d)	75.2 (d)	75.3 (d)	75.3 (d)	75.2 (d)	75.2 (d)	75.2 (d)	75.3 (d)	75.2 (d)	75.3 (d)	75.2 (d)	75.2 (d)	75.2 (d)	75,3 (d)
3‴	78.4 (d)	78.5 (d)	78.4 (d)	78.5 (d)	78.5 (d)	78.6 (d)	78.5 (d)	78.5 (d)	78.5 (d)	78.6 (d)	78.4 (d)	78.5 (d)	78.5 (d)	78.5 (d)	78.5 (d)	78.6 (d)
4‴	71.6 (d)	71.8 (d)	71.9 (d)	71.8 (d)	71.8 (d)	71.8 (d)	71.8 (d)	71.8 (d)	71.8 (d)	72.0 (d)	71.9 (d)	71.8 (d)	71.8 (d)	71.7 (d)	71.8 (d)	71.9 (d)
5‴	78.4 (d)	78.5 (d)	78.3 (d)	78.4 (d)	78.5 (d)	76.6 (d)	78.4 (d)	78.4 (d)	78.6 (d)	78.5 (d)	78.6 (d)	78.4 (d)	78.5 (d)	78.3 (d)	78.5 (d)	78.5 (d)
6‴	62.7 (t)	62.9 (t)	62.8 (t)	62.8 (t)	62.9 (t)	62.9 (t)	62.9 (t)	62.8 (t)	62.9 (t)	62.9 (t)	62.9 (t)	62.9 (t)	62.8 (t)	62.8 (t)	62.9 (t)	62.9 (t)

Multiplicities were determined by distortionless enhancement by polarization transfer (DEPT) (method: relaxation delay 1.000 sec; pulse 90.0 degree; acquisition time 1.300 sec; observed ^{13}C (125.7 MHz); decouple ^{1}H (499.9 MHz); 640 repetitions; total time 99 minutes)

Signals were assigned from the heteronuclear multiple quantum coherence (HMQC) and heteronuclear multiple bond coherence (HMBC) spectra

3β-O-(4-O-Gentiobiosyl-D-diginosyl)-14α-hydroxy-8-oxo-8,14-seco-5β-card-20(22)-enolide.[15] **14** was obtained as a colorless powder; mp 185°–189°C (acetone–hexane); $[\alpha]_D^{20}$ –11.3° (*c* 0.515, MeOH). IR (KBr): ν_{max} cm^{-1} 3514, 1745.

3β-O-(4-O-gentiobiosyl-D-diginosyl)-14-oxo-15(15→8) abeo-card-20(22)-enolide.[16] **15** was obtained as a colorless powder; mp 184°–186°C (acetone–hexane); $[\alpha]_D^{20}$ +14.6° (*c* 0.125, MeOH); IR (KBr): ν_{max} cm^{-1} 3403, 1747.

Inhibitory activity on induction of intercellular adhesion molecule-1 (ICAM-1)

Cells. Human lung carcinoma A549 cells were provided by the Heath Science Research Resources Bank (Tokyo, Japan). A549 cells were maintained in RPMI 1640 medium (Invitrogen, Carlsbad, CA) supplemented with 10% (v/v) fetal calf serum (JRH Bioscience, Lenexa, KS) and a penicillin–streptomycin–neomycin antibiotic mixture (Invitrogen).

Reagent. Mouse anti-human ICAM-1 antibody (clone 15.2) was purchased from Leinco (St. Louis, MO), and peroxidase-conjugated goat anti-mouse IgG antibody was obtained from Jackson ImmunoResearch (West-Grove, PA, USA). Recombinant human IL-1α and TNF-α were kindly provided by Dainippon Pharmaceutical Co. Ltd. (Osaka, Japan).

Procedures. A549 cells were seeded in a microtiter plate at 2×10^4 cells/well the day before the assay. After A549 cells were pretreated with or without test compounds in 75 µl for 1 h, 25 µl of IL-1α (1 ng/ml) or TNF-α (10 ng/ml) were added to the culture, and the cells were further incubated for 6 h. The cells were washed once with phosphate-buffered saline (PBS) and fixed by incubation with 1% paraformaldehyde–PBS for 15 min and then washed once with PBS. After blocking with 1% bovine serum albumin–PBS overnight, the fixed cells were treated with mouse anti-human ICAM-1 antibody for 60 min. After being washed three times with 0.02% Tween 20–PBS, the cells were treated with horseradish peroxidase-linked anti-mouse IgG antibody for 60 min. The cells were washed three times with 0.02% Tween 20–PBS. The cells were incubated with the substrate (0.1% *o*-phenylenediamine dihydrochloride and 0.02% H_2O_2 in 0.2 M sodium citrate buffer, pH 5.3) for 20 min at 37°C in the dark and assayed for absorbance at 415 nm by using a microplate reader. Expression of ICAM-1 was calculated as follows:

Expression of ICAM-1 (% of control) = [(absorbance with sample and cytokine treatment – absorbance without cytokine treatment)/(absorbance with cytokine treatment – absorbance without cytokine treatment)] × 100

Cell viability. A549 cells (2×10^4 cells/well) were seeded in a microtiter plate the day before the assay and incubated in the presence or absence of test compounds for 24 h. For the last 4 h of induction, the cells were pulsed with 500 µg/ml of 3-(4,5-dimethylthiazo-2-yl)-2,5-diphenyl tetrazolium bromide (MTT). MTT formazan was solubilized with 5% sodium dodecyl sulfate (SDS) overnight. Absorbance at 595 nm was measured and cell viability (%) was calculated as follows:

Cell viability (%) = [(experimental absorbance – background absorbance)/(control absorbance – background absorbance)] × 100

Cell growth inhibitory activity of compounds to WI-38 fibroblast cells, VA-13 malignant tumor cells, and HepG2 human liver tumor cells in vitro

Experimental details were described in a previous article.[17]

Cellular accumulation of calcein

Cells. Adriamycin-resistant human ovarian cancer A2780 cells (AD10) were maintained in RPMI 1640 medium (Invitrogen) supplemented with 10% (v/v) FBS (Fitron, Australia) with 80 µg/ml kanamycin.

Procedures. Medium (100 µl) containing ca. 1×10^6 cells was incubated at 37°C in a humidified atmosphere containing 5% CO_2 for 24 h. Test compounds were dissolved in dimethyl sulfoxide and diluted with phosphate-buffered saline, PBS (–). Test samples (50 µl) were added to the medium and incubated for 15 min. Then, 50 µl of the fluorogenic dye calcein acetoxymethyl ester (AM) [1 µl in PBS (–)]was added to the medium, and incubation was continued for a further 60 min. After removing the supernatant, each microplate was washed with 200 µl of cold PBS (–). The washing step was carried out three times and 200 ml of cold PBS (–) was added. Retention of the resulting calcein was measured as calcein-specific florescence. The absorption maximum for calcein is 494 nm and the emission maximum is 517 nm.

Results and discussion

In vitro anti-inflammatory activity

Expression of ICAM-1 is induced by interleukin-1 (IL-1) and tumor necrosis factor-α(TNF-α) on the surface of endothelial cells of blood vessels. The interaction between ICAM-1 expressed on vascular endothelium and its counterpart lymphocyte function-associated antigen-1 (LFA-1) on leukocytes plays an essential role in the transendothelial migration of leukocytes into inflammation sites.[18] Attacks from leukocytes cause serious damage to inflammatory tissue. Inflammatory cytokines such as IL-1 and TNF-α target neighboring endothelial cells to activate the NF-κB signaling pathway that induces a variety of genes, including ICAM-1.[19] Expression of excess ICAM-1 on the surface of activated endothelial cells of blood vessel plays an important role in the progress of the inflammatory reaction. These facts suggest that an inhibitor of induction of ICAM-1 may

Table 2. Effect of compounds on induction of intercellular adhesion molecule-1 (ICAM-1) and on cell viability (IC_{50}, μM)

Assay	1	2	3	4	5	6	7	8	9	10	11	12	13	14	15	16
IL-1α[a,b]	5.31	3.16	4.71	6.54	1.69	65.4	34.3	>316	67.8	>316	78.1	36.2	66.6	53.6	>316	150
TNF-α[a,b]	3.40	2.01	2.48	3.29	1.20	46.0	25.2	>316	44.5	203	62.2	25.7	49.0	36.5	149	66.2
Cell viability by MTT assay[c,d]	>316	>316	>316	>316	>316	>316	>316	>316	>316	>316	>316	>316	>316	>316	>316	>316

MTT, 3-(4,5-dimethylthiazo-2-yl)-2,5-diphenyl tetrazolium bromide

[a] IC_{50} was calculated using the following equation. Expression of ICAM-1 (% of control) = [(absorbance with sample and IL-1α/TNF-α treatment − absorbance without IL-1α/TNF-α treatment)/(absorbance with IL-1α/TNF-α treatment − absorbance without IL-1α/TNF-α treatment)] × 100. IC_{50} values are means of two independent experiments except for **16**

[b] A549 cells (2×10^4 cells/well) were pretreated with various concentrations of the compounds for 1 h and then incubated in the presence of IL-1α or TNF-α for 6 h. Absorbance of 415 nm was assayed after treatment of the cells with primary and secondary antibodies and addition of the enzyme substrate. The experiments were carried out in triplicate cultures

[c] IC_{50} was determined using the following equation. Cell viability (%) = [(experimental absorbance − background absorbance)/(control absorbance − background absorbance)] × 100. The representative IC_{50} of two independent experiments are shown except for **16**

[d] A549 cells were incubated with serial dilutions of the compounds for 24 h. Cell viability (%) was measured by MTT assay

The experiments were carried out in triplicate cultures

turn out to yield a new type of anti-inflammatory agent. With this in mind, we began to examine compounds **1**–**16** to determine their inhibitory activities on the induction of ICAM-1 through bioassays. The in vitro anti-inflammatory activity of isolated compounds **1**–**16** was estimated by inhibition of the induction of ICAM-1 in the presence of IL-1α and TNF-α[20–22] using human cultured cell line A549 cells, an in vitro human endothelial cell model. Cell viability was measured by MTT assay (Table 2). The assay results of **1**–**16** are summarized as follows: (1) The 14-hydroxy-5β,14β-card-20(22)-enolide structure is important for the inhibitory activity on the induction of ICAM-1, such as that shown for **1**–**5**. (2) Among these, 3β-*O*-(4-*O*-gentiobiosyl-L-oleandrosyl)-16β-acetoxy-14-hydroxy-5β,14β-card-20(22)-enolide (**5**) is the most effective compound. Since **5** showed very weak cytotoxic activity (IC_{50} > 316 μM), it may be a potentially desirable anti-inflammatory agent. (3) Structural changes at C-3 of **5** from 3β-*O*-(4-*O*-gentiobiosyl-L-oleandrosyl) to 3β-*O*-(4-*O*-gentiobiosyl-D-diginosyl) or 3β-O-(4-*O*-gentiobiosyl-D-digitalosyl) did not result in as great a change in activity as similar changes in **3** and **4** did. (4) Elimination of an acetoxy group at C-16 in **3** and **4** did not induce as great a change in activity as similar eliminations in the corresponding compounds **1** and **2** did. (5) Introduction of an additional hydroxyl group at C-8 in **1** to **13** or a change of the 14-hydroxy group of **2** to the 8,14-epoxide ring of **9** led to a large decrease in activity. Changing the 14-hydroxy group of **1** to the 8,14-epoxide ring of **8** led to a loss of activity. (6) The change of the 5β,14β-card-20(22)-enolide structure of **1** and **2** to the corresponding 5α,14β-card-20(22)-enolide structure of **6** and **7** led to a large decrease of activity. (7) Introduction of an epoxide ring at the 7,8 position of **1** led to as large a decrease of activity as that shown for **16**. In conclusion, 14-hydroxy-5β,14β-card-20(22)-enolide is the essential structure for the inhibitory activity of induction of ICAM-1. Introduction of one more hydroxy group at C-8 or C-16 or the change of the 14-hydroxy group to an 8,14-epoxy group led to a large decrease of activity, as shown in **13**, **12**, and **9,** or the loss of activity, as shown in **8**. Introduction of a new epoxide ring at the 7β,8β position of **1** also led to a large decrease of activity in **16**. Compounds **1**–**7** and **9**–**16** showed inhibitory activity on the induction of ICAM-1 induced by IL-1α and TNF-α at roughly the same level. These results suggest that the compounds block the common signaling pathway of NF-κB activation downstream of IκB kinase activation, the de novo RNA/protein synthesis of ICAM-1, or its intracellular transport to the plasma membrane.

Table 3. Cell growth inhibitory activities of compounds against WI-38, VA-13, and HepG2 cells

Compound	IC_{50} (μM)[a]		
	WI-38	VA-13	HepG2
1	3.32	7.06	3.06
2	3.93	10.9	4.00
3	7.20	9.80	4.90
4	3.16	13.8	6.00
5	0.56	5.88	2.71
6	78.3	97.5	66.4
7	68.5	99.1	39.9
8	>100	>100	>100
9	86.5	>100	69.3
10	>100	>100	>100
11	84.8	>100	63.1
12	14.3	69.1	25.8
13	48.2	94.7	37.0
14	9.66	60.2	43.4
15	77.4	>100	96.9
16	64.8	88.2	65.9
Paclitaxel	0.19	0.038	1.48
Adriamycin	2.38	0.18	0.40

[a] IC_{50} values are the means of duplicate determinations

Cytotoxic activities of compounds toward human cancer and normal cells

Cytotoxic activities of **1**–**16** were evaluated against three cell lines: WI-38 fibroblast cells, VA-13 malignant tumor cells, and HepG2 human liver tumor cells (Table 3). The results for **1**–**16** are summarized as follows: (1) The 14-hydroxy-5β,14β-card-20(22)-enolide structure is important for the cell growth inhibitory activity of cardenolides. Thus compounds **1** and **2**, with 14-hydroxy-5β,14β-card-20(22)-enolide functionalities, showed stronger activities

toward WI-38, VA-13, and HepG2 cells than those of the corresponding compounds **6** and **7** with 14-hydroxy-5α,14β-card-20(22)-enolide functions. (2) 3β-*O*-(4-*O*-Gentiobiosyl-L-oleandrosyl)-16β-acetoxy-14-hydroxy-5β,14β-card-20(22)-enolide (**5**) is the most effective compound toward WI-38, VA-13, and HepG2 cells. Its 3β-*O*-(4-*O*-gentiobiosyl-D-diginosyl) derivative (**3**) and 3β-*O*-(4-*O*-gentiobiosyl-D-digitalosyl) derivative (**4**) also showed strong activity toward HepG2. (3) Change of the functional group of **1** from the 14-hydroxy group to the 8,14-epoxy group led to the loss of activity, as shown by the IC_{50} value (>100 μM) of **8**. Change of the functional group of **2** from the 14-hydroxy group to the 8,14-epoxy group led to a large decrease of activity toward WI-38 and HepG2 and the loss of activity toward VA-13, as shown by the IC_{50} values of **9**. (4) Introduction of an additional hydroxyl group at C-8 in **1** led to a large decrease of activity, as shown by the increase in the IC_{50} values of **13**. (5) Introduction of a new epoxide ring in the 7β,8β position of **1** also led to a large decrease of activity, as shown by the increase of the IC_{50} values of **16**. (6) Change of the functional group at C-16 of **5** from a 16-acetoxy group to a 16-hydroxy group led to a large decrease of activity, as shown by the increase in the IC_{50} values of **12**. In conclusion, 14-hydroxy-5β,14β-card-20(22)-enolide is the essential structure for expression of cytotoxic activity toward WI-38, VA-13, and HepG2. Introduction of one more hydroxy group at C-8 or C-16, a new epoxide ring at the 7β,8β position, or the change of the 14-hydroxy group to a 8,14-epoxy group led to a large decrease of activity or the loss of activity, as shown in **8** and **10**.

MDR-cancer reversal activity of compounds

In cancer chemotherapy, the occurrence of multidrug resistance (MDR) in cancer cells caused by repeated administration of anticancer agents is a serious problem. One mechanism of MDR is overexpression of P-glycoprotein (P-gp), which is the efflux pump of anticancer drugs.[23–25] P-gp is a transporter for a wide range of reagents utilizing energy by hydrolysis of ATP. When P-gp is expressed on the cell membrane of cancer cell, it transports various kinds of anticancer agents from inside the cell to the outside. We estimated the effects of cardenolide triglycosides **1**–**16** as MDR reversal agents by measuring the increase of cellular accumulation of the fluorogenic dye calcein, which was derived from calcein AM in the course of the assay by enzymatic hydrolysis inside the cell and was used as an effective functional fluorescent probe for the drug efflux protein. We assayed the increase of cellular accumulation of calcein in MDR human ovarian cancer 2780AD cells. The effects of cardenolide triglycoside derivatives **1**–**16** on the cellular accumulation of calcein in MDR human ovarian cancer 2780AD cells were examined. Compounds **9**–**11** and **13**–**15** showed weak to moderate effects on the accumulation of calcein in MDR 2780AD cells in comparison with the control (Tables 4–8). It is interesting to note that the cytotoxic activities of compounds **13** and **14** toward HepG2 were moderate in addition to the significant effect on the accu-

Table 4. Effect of compounds **1**, **2**, and **8** on accumulation of calcein in MDR 2780AD cells

Compound	Concentration[a] (μg/ml)	Average fluorescence/well[b]	±SD	Percentage of control[c]
Control	0	2373	77	
1	0.25	2683	463	113
	2.5	2331	149	98
	25	1920	85	81
2	0.25	2325	152	98
	2.5	2193	268	92
	25	1880	83	79
8	0.25	2360	164	99
	2.5	2255	28	95
	25	2209	206	93

[a]The amount of calcein accumulated in multidrug-resistant human ovarian cancer 2780AD cells was determined with the control in the presence of 0.25, 2.5, and 25 μg/ml of compounds
[b]Values represent means of triplicate experiments
[c]Values are relative amount of calcein accumulated in the cell compared with the control

Table 5. Effect of compounds **3**, **12**, and **13** on accumulation of calcein in MDR 2780AD cells

Compound	Concentration[a] (μg/ml)	Average fluorescence/well[b]	±SD	Percentage of control[c]
Control	0	3456	352	
3	0.25	2966	460	86
	2.5	3045	535	88
	25	2591	299	75
12	0.25	3200	31	93
	2.5	3499	420	101
	25	2298	386	66
13	0.25	3611	78	104
	2.5	3505	364	101
	25	4044	72	117

[a]The amount of calcein accumulated in multidrug-resistant human ovarian cancer 2780AD cells was determined with the control in the presence of 0.25, 2.5, and 25 μg/ml of compounds
[b]Values represent means of triplicate experiments
[c]Values are relative amount of calcein accumulated in the cell compared with the control

Table 6. Effect of compounds **4** and **15** on accumulation of calcein in MDR 2780AD cells

Compound	Concentration[a] (μg/ml)	Average fluorescence/well[b]	±SD	Percentage of control[c]
Control	0	2448	66	
4	0.25	2747	225	112
	2.5	2528	284	103
	25	2300	35	94
15	0.25	2658	440	108
	2.5	2588	331	106
	25	2511	202	103

[a]The amount of calcein accumulated in multidrug-resistant human ovarian cancer 2780AD cells was determined with the control in the presence of 0.25, 2.5, and 25 μg/ml of compounds
[b]Values represent means of triplicate experiments
[c]Values are relative amount of calcein accumulated in the cell compared with the control

Table 7. Effect of compounds **5**, **14**, and **16** on accumulation of calcein in MDR 2780AD cells

Compound	Concentration[a] (μg/ml)	Average fluorescence/well[b]	±SD	Percentage of control[c]
Control	0	2211	516	
5	0.25	2311	354	105
	2.5	1995	149	90
	25	1824	465	82
14	0.25	2460	296	111
	2.5	2417	555	109
	25	2592	707	117
Control	0	4376	182	
16	0.25	4083	781	93
	2.5	3977	832	91
	25	4242	585	97

[a]The amount of calcein accumulated in multidrug-resistant human ovarian cancer 2780AD cells was determined with the control in the presence of 0.25, 2.5, and 25 μg/ml of compounds
[b]Values represent means of triplicate experiments
[c]Values are relative amount of calcein accumulated in the cell compared with the control

Table 8. Effect of compounds **6**, **7**, and **9**–**11** on accumulation of calcein in MDR 2780AD cells

Compound	Concentration[a] (μg/ml)	Average fluorescence/well[b]	±SD	Percentage of control[c]
Control	0	4473	335	
6	0.25	4385	54	98
	2.5	4447	288	99
	25	4007	234	90
7	0.25	4802	81	107
	2.5	4556	307	102
	25	3836	422	86
9	0.25	5081	113	114
	2.5	4556	730	102
	25	4649	471	104
10	0.25	4838	401	108
	2.5	4770	60	100
	25	4729	294	106
11	0.25	4269	352	95
	2.5	4294	261	96
	25	4755	154	106

[a]The amount of calcein accumulated in multidrug-resistant human ovarian cancer 2780AD cells was determined with the control in the presence of 0.25, 2.5, and 25 μg/ml of compounds
[b]Values represent means of triplicate experiments
[c]Values are relative amount of calcein accumulated in the cell compared with the control

mulation of calcein in MDR 2780AD. In contrast, compounds **9**–**11** and **15** showed very weak or no cytotoxic activity toward VA-13 and HepG2. Thus, compounds **9**–**11** and **15** are possible lead compounds for MDR cancer reversal agents and compounds **13** and **14** are expected to be lead compounds in development of anti-MDR cancer agents.

Conclusion

3*β*-*O*-(4-*O*-Gentiobiosyl-L-oleandrosyl)-16*β*-acetoxy-14-hydroxy-5*β*,14*β*-card-20(22)-enolide (**5**) showed the most effective inhibitory activity of induction of ICAM-1 as well as the most effective cytotoxic activity toward WI-38, VA-13, and HepG2 among cardenolide triglycosides **1**–**16** isolated from *N. oleander*. Analogously, compounds **1**–**4,** with modified 14-hydroxy-5*β*,14*β*-card-20(22)-enolide structures, showed significant inhibitory activity of induction of ICAM-1 as well as effective cytotoxic activity toward WI-38, VA-13, and HepG2. Thus, the 14-hydroxy-5*β*,14*β*-card-20(22)-enolide structure is the essential structure with or without an acetoxy group at C-16 for the expression of these biological activities. Introduction of a hydroxy group at the C-8 or C-16 positions or displacement of the 14-hydroxy group with an 8,14-epoxy group in the 14-hydroxy-5*β*,14*β*-card-20(22)-enolide structure induced a large decrease in activity or a complete loss of activity. Compounds **13** (with an 8,14-hydroxy-5*β*,14*β*-card-20(22)-enolide structure) and **14** (with a 14*α*-hydroxy-8-oxo-8,14-seco-5*β*-card-20(22)-enolide structure) showed significant effects on the accumulation of calcein in MDR 2780AD cells in addition to moderate cytotoxic activity toward HepG2. Thus, compounds **13** and **14** are expected to be lead compounds in the development of an anti-MDR cancer agent.

Acknowledgments We thank Ms. Seiko Oka and Ms. Hiroko Tsushima of the Center for Instrumental Analysis, Hokkaido University, for obtaining high resolution fast atom bombardment mass (HRFABMS). This work was supported by the Natural Science Foundation of Heilongjiang Province of China (LC2009C12).

References

1. Fieser LF, Fiser M (1959) Steroid. Reinhold, New York, p 727
2. Hong BC, Kim S, Kim TS, Corey EJ (2006) Synthesis and properties of several isomers of the cardioactive steroid ouabain. Tetrahedron Lett 47:2711–2715
3. López-Lázaro M, Pastor N, Azrak SS, Ayuso MJ, Austin CA, Cortés F (2005) Digitoxin inhibits the growth of cancer cell lines at concentrations commonly found in cardiac patients. 68:1642–1645
4. Roy MC, Chang FR, Huang HC, Chiang MYN, Wu YC (2005) Cytotoxic principles from the formosan milkweed, *Asclepias curassavica.* J Nat Prod 68:1494–1499
5. Zhao M, Bai L, Wang L, Toki A, Hasegawa T, Kikuchi M, Abe M, Sakai J, Hasegawa R, Bai Y, Mitsui T, Ogura H, Kataoka T, Oka S, Tsushima H, Kiuchi M, Hirose K, Tomida A, Tsuruo T, Ando M (2007) Bioactive cardenolides from the stems and twigs of *Nerium oleander*. J Nat Prod 70:1098–1103
6. Bai L, Wang L, Zhao M, Toki A, Hasegawa T, Ogura H, Kataoka T, Hirose K, Sakai J, Bai J, Ando M (2007) Bioactive pregnanes from *Nerium oleander*. J Nat Prod 70:14–18
7. Bai L, Hasegawa, R, Hirose K, Ando M, Sakai J, Ando M (2009) A New cardenolide triglycoside from stems and twigs of *Nerium oleander*. Heterocycles 78:2361–2367
8. Yamauchi T, Takata N, Miura T (1975) Cardiac glycosides of the leaves of *Nerium odorum*. Phytochemistry 14:1379–1382
9. Hill RA, Kirk DN, Makin HLJ, Murphy GM (1991) Dictionary of steroids. Chapman and Hall, London, p 237
10. Hanada R, Abe F, Yamauchi T (1992) Steroid glycosides from the root of *Nerium odorum*. Phytochemistry 31:3183–3187
11. Rangaswami VS, Reichstein T (1949) Die glycoside von *Nerium odorum* Sol. I. Pharm Acta Helv 24:159–183
12. Abe F, Yamauchi T (1992) Cardenolides steroids of *oleander* leaves. Phytochemistry 31:2459–2463
13. Yamauchi T, Takahashi M, Abe F (1976) Cardiac glycosides of the root bark of *Nerium odorum.* Phytochemistry 15:1275–1278

14. Rittel W, Reichstein T (1954) Odoroside K and odorobioside K. Die glycoside von *Nerium odorum* Sol. Hel Chim Acta 37: 1361–1373
15. Yamauchi T, Abe F (1978) Neriaside, a 8,14-seco-cardenolide in *Nerium odorum*. Tetrahedron Lett 19:1825–1828
16. Abe F, Yamauchi T (1979) Oleasides; novel cardenolides with an unusual framework in *Nerium* (Nerium 10). Chem Pharm Bull 27:1604–1610
17. Wang L, Bai L, Tokunaga D, Watanabe Y, Hasegawa, T, Sakai J, Tang W, Bai Y, Hirose K, Yamori T, Tomida A, Tsuruo T, Ando M (2008) The polar neutral and basic taxoids isolated from needles and twigs of *Taxus cuspidata* and their biological activity. J Wood Sci 54: 390–401
18. Pober JS, Cotran RS (1990) Cytokines and endothelial cell biology. Physiol Rev 70:427–451
19. Baeuerle PA, Henkel T (1994) Function and activation of NF-κB in the immune system. Annu Rev Immunol 12:141–179
20. Kawai K, Kataoka T, Sugimoto H, Nakamura A, Kobayashi T, Arao K, Higuchi Y, Ando M, Nagai K (2000) Santonin-related compound 2 inhibits the expression of ICAM-1 in response to IL-1 stimulation by blocking the signaling pathway upstream of I*k*B degradation. Immunopharmacology 48:129–135
21. Yuuya S, Hagiwara H, Suzuki T, Ando M, Yamada A, Suda K, Kataoka T, Nagai K (1999) Guaianolides as immunomodulators. Synthesis and biological activities of dehydrocostus lactone, mokko lactone, eremanthin, and their derivatives. J Nat Prod 62: 22–30
22. Zhang S, Zhao M, Bai L, Hasegawa T, Wang J, Wang L, Xue H, Deng Q, Xing F, Bai Y, Sakai J, Bai J, Koyanagi R, Tsukumo Y, Kataoka T, Nagai K, Hirose K, Ando M (2006) Bioactive guaianolides from siyekucai (*Ixeris chinensis*). J Nat Prod 69:1425–1428
23. Ueda K, Cardarelli C, Gottesman MM, Pastan I (1987) Expression of a full-length cDNA for the human "MDR1" gene confers resistance to colchicine, doxorubicin, and vinblastine. Proc Natl Acad Sci USA 84:3004–3008
24. Ueda K, Komano T (1988) The multidrug-resistance gene MDR1. Jpn J Cancer Chemother 15:2858–2862
25. Tsuruo T, Iida-Saito H, Kawabata H, Oh-hara T, Hamada H, Utakoji T (1986) Characteristics of resistance to adriamycin in human myelogenous leukemia K 562 resistant to adriamycin and in isolated clones. Jpn J Cancer Res 77:682–692